Quantitative Nuclear Proteomics Identifies mTOR Regulation of DNA Damage Response*[S]

Sricharan Bandhakavi‡§, Young-Mi Kim‡§, Seung-Hyun Ro‡, Hongwei Xie‡, Getiria Onsongo¶, Chang-Bong Jun‡, Do-Hyung Kim‡‖, and Timothy J. Griffin‡**

Cellular nutritional and energy status regulates a wide range of nuclear processes important for cell growth, survival, and metabolic homeostasis. Mammalian target of rapamycin (mTOR) plays a key role in the cellular responses to nutrients. However, the nuclear processes governed by mTOR have not been clearly defined. Using isobaric peptide tagging coupled with linear ion trap mass spectrometry, we performed quantitative proteomics analysis to identify nuclear processes in human cells under control of mTOR. Within 3 h of inhibiting mTOR with rapamycin in HeLa cells, we observed down-regulation of nuclear abundance of many proteins involved in translation and RNA modification. Unexpectedly, mTOR inhibition also down-regulated several proteins functioning in chromosomal integrity and up-regulated those involved in DNA damage responses (DDRs) such as 53BP1. Consistent with these proteomic changes and DDR activation, mTOR inhibition enhanced interaction between 53BP1 and p53 and increased phosphorylation of ataxia telangiectasia mutated (ATM) kinase substrates. ATM substrate phosphorylation was also induced by inhibiting protein synthesis and suppressed by inhibiting proteasomal activity, suggesting that mTOR inhibition reduces steady-state (abundance) levels of proteins that function in cellular pathways of DDR activation. Finally, rapamycin-induced changes led to increased survival after radiation exposure in HeLa cells. These findings reveal a novel functional link between mTOR and DDR pathways in the nucleus potentially operating as a survival mechanism against unfavorable growth conditions. ***Molecular & Cellular Proteomics 9:403–414, 2010.***

Eukaryotic cells coordinately regulate molecular processes in distinct subcellular compartments for growth and survival in response to nutritional status and environmental stress. A crucial integrator/coordinator for these cellular responses is mTOR,[1] a nutrient-responsive protein kinase belonging to the phosphatidylinositol kinase-related kinase family (1). mTOR, as a downstream element of the insulin/IGF-1-phosphoinositide 3-kinase-Akt pathway, plays an important role in the regulation of a variety of cellular processes in response to nutrient and growth factor signals (1, 2). mTOR is mainly known for its regulation of translation and protein synthesis, and it is also involved in the regulation of diverse cellular and biological processes such as cell cycle progression, actin cytoskeleton rearrangement, transcription, autophagy, and development (1, 2). Despite the pervasive role of mTOR in different cellular functions, its ability to coordinately regulate diverse processes in distinct cellular compartments, particularly those occurring in the nucleus of mammalian cells, remains poorly defined.

There has been growing evidence that TOR regulates diverse processes in the nucleus. In *Saccharomyces cerevisiae*, TOR regulates the nucleocytoplasmic shuttling of several transcription factors (1, 3). TOR complex 1, TORC1, itself undergoes translocation to the nucleus and interacts with chromatin-modifying factors within ribosomal RNA and subtelomeric loci to regulate the expression of ribosomal RNAs and proteins and amino acid transporters (4). Microarray analyses in *Drosophila* and mammalian cells revealed a key role for TOR in regulating the expression of nuclear proteins involved in cell growth (5–7). mTOR, like the yeast TOR1/2, undergoes nucleocytoplasmic shuttling, and the nuclear localization was shown to be important to phosphorylate downstream substrates, such as S6K and 4E-BP1 (8, 9). A recent study showed that nuclear mTOR interacts with the promyelocytic leukemia tumor suppressor under hypoxic conditions to down-regulate mTOR signaling and neoangiogenesis in

From the Departments of ‡Biochemistry, Molecular Biology, and Biophysics and ¶Computer Science and Engineering, University of Minnesota, Minneapolis, Minnesota 55455

Received, July 20, 2009, and in revised form, November 19, 2009
Published, MCP Papers in Press, November 23, 2009, DOI 10.1074/mcp.M900326-MCP200

[1] The abbreviations used are: mTOR, mammalian target of rapamycin; TOR, target of rapamycin; iTRAQ, isobaric tags for relative and absolute quantification; PQD, pulsed Q dissociation; DDR, DNA damage response; IR, ionizing radiation; LTQ, linear trap quadrupole; ATM, ataxia telangiectasia mutated; SCX, strong cation exchange; ATR, ATM and Rad3-related kinase; AMPK, AMP-activated protein kinase; TERT, telomerase reverse transcriptase; GFP, green fluorescent protein; siRNA, short interfering RNA; NPM, nucleophosmin; PTBP, polypyrimidine tract-binding protein; ROD1, regulator of differentiation 1; TNKS1BP1, tankyrase 1-binding protein 1; Gy, gray; UTR, untranslated region.

mouse and human tumors (10). mTOR also controls nuclear localization of a few transcriptional regulators involved in cellular stress responses and rRNA expression (9, 11–13).

Although these studies have indicated important roles for mTOR in the regulation of nuclear events, the diversity of nuclear functions under its control and how they are coordinated with other roles of mTOR remain poorly understood. Elucidating these functions would benefit from system-wide analysis, such as mass spectrometry-based quantitative proteomics, which has particular value for identifying post-transcriptional changes that are not predicted using genomics/transcriptomics methods (14–16). Maturing protein preparation methods and mass spectrometry instrumentation (17), combined with subcellular fractionation, have made possible discoveries of important regulatory events in organelles within cells. However, such methods have not yet been applied to studies on nutrient and mTOR regulation of nuclear or other subcellular events.

In this study, we sought to profile nuclear proteins regulated by mTOR using a recently developed method that combines the robustness of an LTQ linear ion trap mass spectrometer operated in pulsed Q dissociation (PQD) mode with isobaric peptide labeling using the iTRAQ reagent (18). Our analysis identified 48 proteins whose abundance in the nucleus is altered by rapamycin in HeLa cells. Independent validation confirmed that mTOR regulates nuclear abundance of proteins involved in protein synthesis, RNA modification, and, unexpectedly, chromosomal integrity and DNA damage responses (DDRs). Consistent with these proteomic changes, downstream analysis determined that rapamycin or mTOR knockdown activates ataxia telangiectasia mutated (ATM)/DDR signaling. Rapamycin-induced ATM activation was mimicked by inhibition of protein synthesis and suppressed by inhibition of proteasomal function. Finally, we identified that the rapamycin-induced changes are important for cell survival upon exposure to DNA-damaging conditions, such as ionizing radiation (IR). Our results demonstrate the value of subcellular quantitative proteomics for unraveling post-transcriptional regulation and identifying novel mTOR functions within a complex subcellular compartment.

EXPERIMENTAL PROCEDURES

Isolation of Nuclear and Cytoplasmic Fractions—Purified nuclei were obtained from HeLa cells treated with rapamycin or vehicle for 3 h. Cells were harvested by trypsin; washed in PBS, low salt buffer (buffer A: 10 mM HEPES, pH 7.9, 1.5 mM $MgCl_2$, 10 mM NaCl, 0.5 mM DTT); and allowed to swell in buffer A supplemented with protease inhibitor mixture (Roche Applied Science) for 15 min. Prior to homogenization, Nonidet P-40 was added to a final concentration of 0.3%, and cells were lysed in a prechilled Dounce homogenizer with 20 strokes using a tight pestle. This mixture was centrifuged at 228 × *g* to obtain a crude nuclear pellet and cytoplasmic supernatant. The nuclear pellet was resuspended in low sucrose buffer containing 0.3 M sucrose, 10 mM HEPES, pH 7.9, 5 mM $MgCl_2$, 10 mM NaCl and layered over 3 volumes of the same buffer supplemented to 1.8 M sucrose followed by centrifugation at 25,000 × *g* for 35 min. The highly pure nuclear pellet was extracted with buffer A supplemented with 0.42 M NaCl, 0.3 M sucrose, 0.5% Triton X-100 twice, and the extracted protein was processed for proteomics analysis.

iTRAQ Labeling and Proteomics Analysis—Nuclear protein samples were acetone-precipitated and dissolved in iTRAQ dissolution buffer. 100 μg of protein from each sample was trypsinized, labeled with iTRAQ reagents 114 (non-rapamycin treated sample) and 115 (rapamycin-treated sample). Labeled peptides were pooled and fractionated by strong cation exchange (SCX) HPLC. 45 SCX fractions were collected and analyzed using optimized collision energy settings on an LTQ instrument (Thermo Scientific) using pulsed Q dissociation (LTQ-PQD) as described (18).

Protein Identification and Quantification—Obtained MS/MS spectra were searched using SEQUEST (19) (Bioworks version 3.2, Thermo Finnigan, San Jose, CA) against a non-redundant human protein sequence database from the European Bioinformatics Institute (ipi.HUMAN.v3.18.fasta containing 62,000 entries). This database was chosen because it is manually curated to minimize protein redundancy due to identical protein sequences appearing under different accession codes. A reversed sequence version of the same database was appended to the end of the forward version for the purpose of false positive rate estimation (20). Search parameters included static mass shift (+144.0 Da) for the N terminus and lysine due to modification with the iTRAQ reagent. Differential amino acid mass shifts for oxidized methionine (+16 Da) were also included. Precursor peptide mass tolerance was ±2.0 Da with partial tryptic specificity. Fragment ion tolerance was set at 1.0 Da. The search results were validated using the peptide validation program PeptideProphet (21), which assigns a comprehensive probability (*p*) score from 0 to 1 to each peptide sequence match based on its SEQUEST scores (Xcorr, ΔCn, Sp, and RSp) and additional information, including mass difference between the precursor ion and the assigned peptide and the number of tryptic termini. The peptide sequence match results were organized and interpreted using the software tool Interact (22), allowing up to two missed cleavage for identified peptides. Peptide matches were filtered using a *p* score threshold of 0.92 for all data sets, ensuring an estimated false positive rate below 1% calculated by reversed database searching. Relative abundance ratios for each identified protein were calculated as described previously (18). iTRAQ ratios of individual proteins were normalized by dividing each ratio by the average -fold change (2.1) calculated across all quantified proteins in the data set.

To report the minimum set of protein sequences in our proteomic catalogue that adequately accounts for all matched peptides, we analyzed all matched peptide sequences for redundant inclusion in multiple proteins in our sequence database. Proteins identified from at least one non-redundant peptide sequence were retained in our catalogue. For proteins identified from redundant peptides, we retained those proteins in our catalogue only if the redundant proteins matched to a closely related isoform of the same protein in the database as determined by manual inspection. Proteins identified from redundant peptides that matched to different proteins entirely were removed.

Antibodies, Chemicals, and Cell Lines—The antibodies used were as follows. Anti-mTOR (sc-1549), anti-p53 (sc-6243), anti-Ku70 (sc-9033), and anti-ATM (sc-7230) antibodies were purchased from Santa Cruz Biotechnology (Santa Cruz, CA). Anti-S6K1 (9202), anti-phospho-S6K1 Thr-389 (9205), anti-phospho-53BP1 Ser-25/29 (2674), anti-phospho-ATM and Rad3-related kinase (ATR) Ser-428 (2853), anti-AMPK (2532), anti-phospho-AMPK Thr-172 (2531S), and anti-phospho-p53 Ser-15 (9284) were from Cell Signaling Technology (Danvers, MA). Anti-53BP1 (A300-272A), anti-eIF3S8 (A300–376A), anti-MDC1 (A300-051A), anti-RPL7A (A300-749A), anti-SMC2 (A300-058A), anti-NCAPD3 (A300-604A), anti-NUP98 (A301-786A), and anti-

H2AX (A300-082A) antibodies were from Bethyl Laboratories (Montgomery, TX). Antibodies against fibrillarin (ab4566), U1A (ab40689), nucleophosmin (ab10530), Histone H1.0 (ab11079), and SNF2L2/hBRM (ab15597) were from Abcam (Cambridge, MA). Anti-53BP1 (DR1003), anti-phospho-H2AX Ser-139 (DR1017), and anti-p53 (OP03) were from Calbiochem. Antibodies against telomerase reverse transcriptase (TERT) (MA3-16571 and NB110-89471) were purchased from Affinity BioReagents (Golden, CO) and Novus (Littleton, CO), respectively. Antibodies against valosin-containing protein (612182) and actin (612656) were purchased from BD Biosciences. Secondary antibodies coupled to AlexaFluor 488 and AlexaFluor 647 were obtained from Invitrogen. Rapamycin (Calbiochem), cycloheximide, and MG132 were used at 50 nM, 50 μM, and 10 μM, respectively. Leucine amino acid starvation was done by rinsing cells in leucine-free RPMI 1640 medium twice and incubating in leucine-free RPMI 1640 medium supplemented with or without 52 μg/ml leucine for 2 h (23). All other reagents were purchased from Sigma unless indicated otherwise. ATM cell lines were a generous gift from Dr. E. Hendrickson's laboratory at the University of Minnesota. HeLa, HEK293T, and WI38 cell lines were obtained from the ATCC (Manassas, VA).

Cell Culture and Transfection—HeLa, HEK293T, and WI38 cells were cultured in Dulbecco's modified Eagle's medium (Invitrogen) supplemented with 10% fetal bovine serum, penicillin, and streptomycin at 37 °C in 5% CO_2. ATM wild type and null lymphoblast cells were grown in RPMI 1640 medium (Invitrogen) containing 15% fetal calf serum. Cells were transfected with DNA constructs to express green fluorescent protein (GFP) fusion protein or short hairpin RNA plasmids using FuGENE 6 (Roche Applied Science) following the manufacturer's protocol. The siRNAs were transiently transfected into HeLa cells using jetSI^{TM}-ENDO (Polyplus transfection). siRNA-transfected cells were harvested 2 or 3 days post-transfection for Western blotting and confocal microscopic analysis. The target sequences for mTOR and S6K1 are 5′-aaccctgcctttgtcatgcct-3′ and 5′-cagctaccatccacacaaata-3′, respectively.

DNA Construction—The DNA constructs for GST- or Myc-tagged recombinant proteins were generated by PCR amplification of cDNA clones obtained from Open Biosystems or the Kazusa Institute in Japan. Amplified DNAs were cloned into pEGFP-C3 or N1 vectors (Clontech) or prk-myc.

Immunoprecipitation and Western Blotting—Total nuclear extracts for Western blotting were prepared by boiling isolated nuclei in SDS sample buffer, whereas cytoplasmic fractions were concentrated using Amicon Ultrafree concentrators and adjusted to the same volume in SDS sample buffer. The same volumes of nuclear and cytoplasmic fractions were loaded for Western blot analysis unless indicated otherwise. Total cell lysates were prepared in RIPA buffer (12.5 mM $NaPO_4$, pH 7.2, 2 mM EDTA, 50 mM NaF, 1.25% Nonidet P-40, 1.25% SDS, 0.1 mM DTT). For immunoprecipitations, HeLa cells were lysed in buffer 1 (20 mM Tris·HCl, pH 8.0, 0.4 M NaCl, 1 mM EDTA, 0.5% Nonidet P-40), and an equal volume of buffer 1 lacking NaCl was added to cell lysates. Immunoprecipitates were isolated using anti-p53 or anti-53BP1 antibodies and washed four times with buffer 1 wash buffer (20 mM Tris·HCl, pH 8.0, 0.2 M NaCl, 1 mM EDTA, 0.5% Nonidet P-40). Proteins were loaded onto Tris-glycine gels, transferred to PVDF membranes, and processed for Western blot analysis.

Quantitative Real Time RT-PCR Analysis—HeLa cells were treated with rapamycin or methanol for the indicated periods of time (1, 2, 3, and 6 h of treatment) and harvested. No significant effects on RNA levels of tested genes were detected at 30 min of rapamycin treatment (data not shown). RNA was isolated using TRIzol (Invitrogen), and cDNA was reverse transcribed. Real time PCR analysis was performed on a Roche Light Cycler 3.5 instrument using the FastStart DNA MasterPlus SYBR Green I kit (Roche Applied Science). Primers used for the PCRs are listed in supplemental Table 3. Cycle thresholds for each gene were normalized to tubulin, and the results were expressed as -fold changes with respect to those obtained with cells treated with methanol as controls.

Confocal Microscopy—For immunofluorescence, HeLa cells treated with rapamycin/vehicle for 3 h were fixed with 4% paraformaldehyde and blocked in a PBS buffer containing 0.1% saponin and 3% BSA. This was followed by incubating with primary antibodies and subsequently with secondary antibodies coupled to AlexaFluor 488 or AlexaFluor 647. TERT staining was performed as described previously (24). Cells were also stained with 4′,6-diamidino-2-phenylindole for the nucleus. Stained cells were mounted in Vectashield (Vector Laboratories, Burlingame, CA), and images were acquired using an Olympus FluoView 1000 IX2 inverted microscope.

Clonogenic Viability Assay—HeLa cells in 6-well plates seeded at 300 cells/well were preincubated for 0, 3, or 24 h with rapamycin (50 nM) or methanol and then irradiated at the indicated doses of IR. After irradiation, cells were refreshed with new medium and maintained for 14 days in the absence of rapamycin. Cells were stained with crystal violet, and the number of colonies on plates was counted. Three experiments were conducted for each condition. Cell lysates were prepared in RIPA buffer after cells were incubated in a 37 °C incubator for 90 min following radiation.

RESULTS

Quantitative Proteomics Analysis via iTRAQ Reagent Labeling and LTQ-PQD Identifies Rapamycin-regulated Nuclear Proteome Changes—We used a quantitative mass spectrometric approach using iTRAQ reagent peptide labeling to identify proteins whose abundance in the nucleus is altered by rapamycin, a classical and specific inhibitor of mTOR function (1, 2) (Fig. 1*a*). Rather than build a definitive catalogue of nuclear proteins affected by rapamycin treatment, our goal was to use quantitative proteomics as a first pass screen from which we could obtain a list of proteins putatively regulated by mTOR and generate new hypotheses for further testing via biochemical and cell biological methods. Therefore, we carried out a single quantitative proteomics analysis on highly pure nuclei isolated from two groups of HeLa cells, one treated with rapamycin and the other treated with methanol as a control for 3 h. Isolated nuclei were determined to be morphologically intact (by phase-contrast microscopy) and highly pure (by Western blotting for nuclear and cytoplasmic marker proteins) as shown in supplemental Fig. 1. Nuclear proteins were trypsinized, labeled with iTRAQ stable isotope-encoded reagents, pooled, and fractionated by SCX HPLC. The peptide fractions were subsequently analyzed by microcapillary reversed-phase LC-MS/MS on a linear ion trap (LTQ) instrument operated in PQD mode using methods we have described previously (18).

We obtained a catalogue of 503 proteins identified from two or more unique peptides along with several hundred more proteins identified by single peptide hits at an estimated false positive rate below 1%. Based on our bioinformatics analysis described below, we selected seven additional proteins identified by single hits, resulting in a final catalogue of 510 total proteins. Supplemental Table 1 shows these proteins along with all relevant identification information and iTRAQ reporter

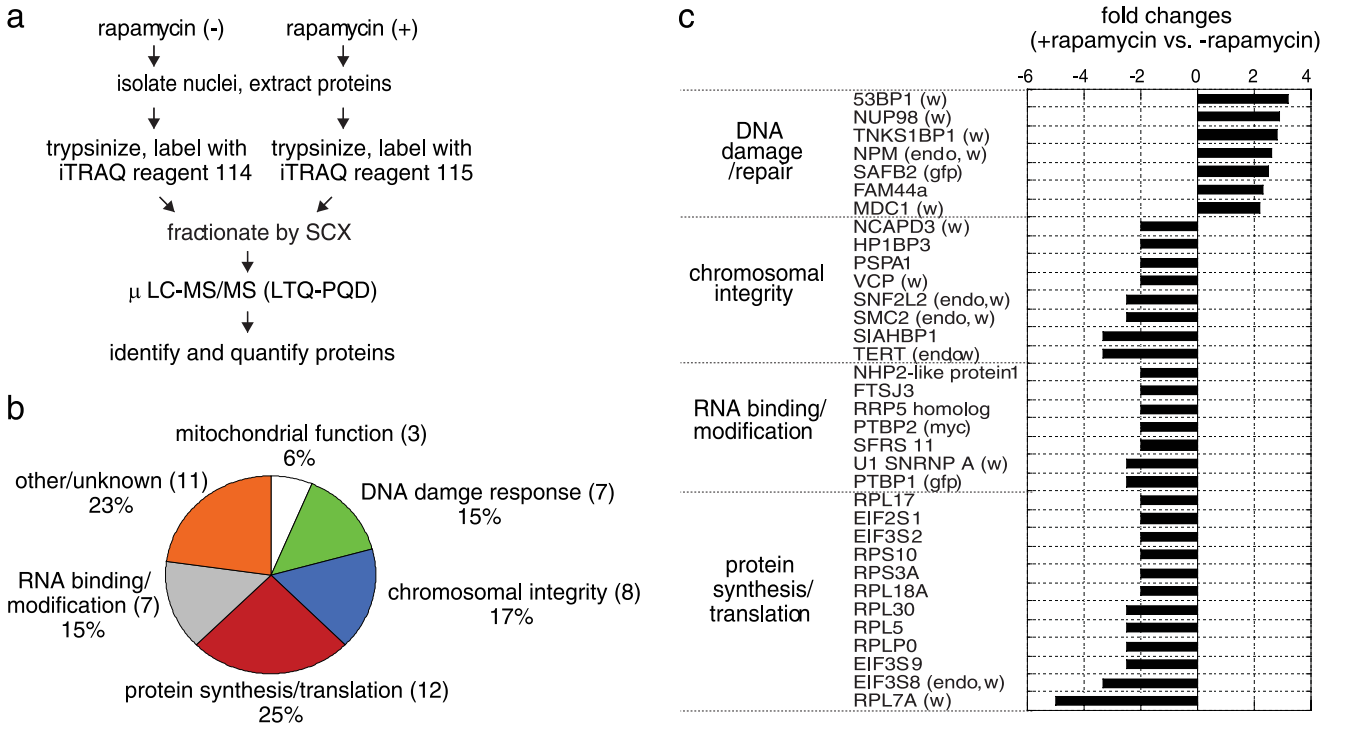

FIG. 1. **Rapamycin induces abundance changes within nuclear proteome of HeLa cells.** *a*, experimental design for quantitative proteomics analysis. For additional details, see "Experimental Procedures." *b*, functional classification of nuclear proteins that changed in nuclear abundance 2-fold or more upon rapamycin treatment. *c*, normalized -fold changes in the levels of rapamycin-regulated proteins. The labels *w*, *endo*, and *gfp* in *parentheses* indicate Western blotting, immunostaining of endogenous proteins, and GFP fluorescence microscopy, respectively, which were used to validate mass spectrometry measurements.

ion intensities. Quantification of the identified proteins was accomplished using a previously described software program, which automatically summed iTRAQ reporter ion intensities derived from centroided MS/MS spectra matched to each protein (18).

Protein ratios were normalized to the average ratio (2.1) calculated across the entire set of proteins to correct for any bias introduced in sample preparation and handling based on the assumption that protein ratios should be centered around unity. Based on previous observations of iTRAQ reagent data on the LTQ, for normalizing our protein abundance ratios, we did not include proteins that showed iTRAQ reporter ion intensities that were below 100 counts as these provide lower confidence quantitative ratios (25). Western blotting of several rapamycin-affected proteins (Fig. 2) supported the corrected ratios as being accurate. We defined proteins as being significantly changed in abundance if they showed a normalized -fold change of at least 2.0 or more as it was significantly outside the calculated standard deviation (0.4) across the set of quantified proteins.

With the goal of generating hypotheses for further testing, we grouped our entire set of identified proteins using Ingenuity Pathway analysis to reveal trends in the functional classes of proteins affected by rapamycin treatment. Using the criteria described above, 48 proteins were selected from our proteomic data set that showed significant changes in their abundance upon rapamycin treatment with most (39 of 48) decreasing in their abundance (supplemental Table 2). Based on their known functions, rapamycin-affected proteins were classified into six functional groups (supplemental Table 2 and Fig. 1*b*): (i) DNA damage/repair (seven proteins), (ii) chromosomal integrity (eight proteins), (iii) RNA binding/modification (seven proteins), (iv) protein synthesis/translation (12 proteins), (v) mitochondrial processes (three proteins), and (vi) other/unknown functions (11 proteins). Most of these proteins (41 of 48 proteins) were identified by two distinct peptides or more. The remaining seven proteins (53BP1, nucleophosmin (NPM), MDC1, FAM44a, NCAPD3, polypyrimidine tract-binding protein 2 (PTBP2), and RPL7A) were identified by a single peptide match. Supplemental Fig. 2 shows the annotated MS/MS spectra matched to these seven proteins. Representative members of DNA damage/repair, chromosomal integrity, RNA binding/modification, and protein synthesis/translation functional categories and their -fold changes upon rapamycin treatment are indicated in Fig. 1*c*.

To confirm the veracity of our proteomic findings overall, abundance changes of selected, representative proteins from each functional category, as well as six of the seven proteins identified by single peptide matches, were independently val-

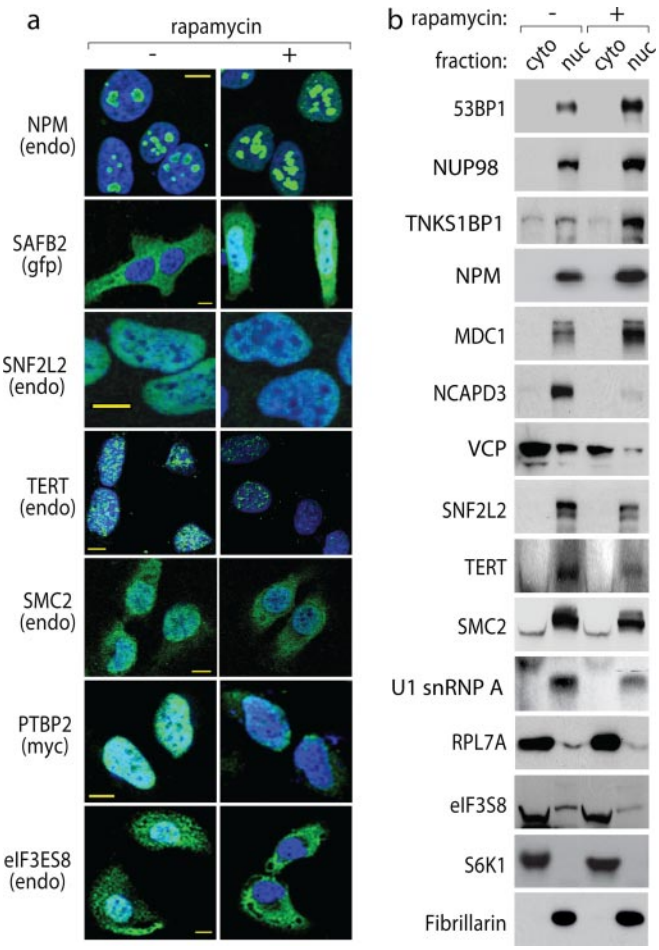

FIG. 2. **Independent validation of proteomic changes across rapamycin-affected functional categories.** *a*, validation of mass spectrometric results performed by immunostaining of endogenous (*endo*) or recombinant proteins (*myc*) or using GFP fluorescence (*gfp*) of transiently expressed proteins. HeLa cells were stained using antibody specific to the indicated proteins (*endo*) or transiently transduced to express GFP-tagged proteins (*gfp*) and visualized by fluorescence microscopy. *b*, validation of mass spectrometric results of nuclear abundance changes in HeLa cells by Western blotting. HeLa cell extracts were separated into cytoplasm (*cyto*) and nuclear (*nuc*) fractions as described under "Experimental Procedures," and their cellular equivalents were loaded on SDS-PAGE prior to Western blotting. S6K1 and fibrillarin levels were monitored for assessing purity of cytoplasmic and nuclear fractions, respectively. *VCP*, valosin-containing protein; *snRNP*, small nuclear ribonucleoprotein.

idated through use of immunofluorescence microscopy and/or Western blotting (Fig. 2, *a* and *b*, and supplemental Figs. 3–5). For all these proteins, the relative abundance levels measured by immunofluorescence and/or Western blotting were consistent with the quantitative proteomics results.

Among functional classes of affected proteins, a few involved in protein synthesis/translation, such as eIF3S8 and RPL7A, and RNA modification, such as PTBP1, might be expected based on the known roles of mTOR (1, 2, 26). Particularly, the decrease of PTBP1 and -2 is consistent with a recent report that they are translocated to the cytoplasm under amino acid starvation (a condition that inhibits mTOR (1, 2)) and relocalized to the nucleus upon supplementation with amino acids (a condition that activates mTOR (1, 2, 26). Because PTBP1 and -2 reduction is predicted to increase expression of their nuclearly localized paralog, regulator of differentiation 1 (ROD1) (27), we tested for potential effect of rapamycin on GFP fusion ROD1 levels. Indeed, we found that rapamycin significantly increased ROD1 levels in the nucleus (supplemental Fig. 4).

An unexpected finding from our proteomics analysis was the effect of rapamycin on proteins involved in DNA modification pathways that regulate DNA damage/repair and chromosomal integrity. 15 of 48 affected proteins were involved in these pathways (supplemental Table 2 and Fig. 1*b*). Independent validation of 11 of these 15 proteins is shown in Fig. 2, *a* and *b*, confirming that rapamycin affected DNA modification pathways regulated by these proteins. Up-regulated proteins included substrates of the DNA damage signaling kinases ATM kinase and ATR (28) (53BP1, FAM44a, and MDC1) and other proteins implicated in DNA damage responses such as tankyrase 1-binding protein 1 (TNKS1BP1), NPM, and NUP98 (29–31). This group also included the multifunctional protein scaffold attachment factor B2 (SAFB2), which has been implicated in coupling transcriptional regulation and cytoskeletal signaling with pre-mRNA splicing and cellular proliferation (32, 33). Down-regulated proteins included TERT (24), the global transcription activator SNF2L2 (34), and the chromatin condensin complex members (35) condensing-2 complex subunit D3 (NCAPD3) and structural maintenance of chromosomal protein 2 (SMC2), which are all involved in chromosomal integrity (Fig. 2, *a* and *b*). We also detected nuclear and cytoplasmic down-regulation of valosin-containing protein (Fig. 2*b*, see the *seventh panel* from the *top*), an Akt substrate involved in nuclear envelope reconstruction, protein degradation pathways, and nuclear inclusion body diseases (36).

Next, we tested the abundance level of mRNAs corresponding to functionally distinct classes of rapamycin-sensitive proteins. With the exception of TNKS1BP1, the remaining proteins were unaffected in regard to the abundance level of their corresponding mRNA transcripts (supplemental Fig. 6). This includes the absence of a significant effect on TERT mRNA (**s**upplemental Fig. 6) or the telomeric RNA component hTR (supplemental Fig. 7). Interestingly, previous studies demonstrated that long term treatment with rapamycin reduced mRNA levels of TERT in distinct cell lines (37, 38); our work indicates earlier reduction of TERT protein abundance in HeLa cells that is independent of mRNA level changes. The analysis of mRNA levels of multiple rapamycin-sensitive proteins indicates significant post-transcriptional regulation in the nucleus by rapamycin and illustrates the value of subcellular quantitative proteomics in identifying such regulatory events.

mTOR Inhibition Activates DDR Pathways—To explain the effect of rapamycin on proteins involved in DNA modification

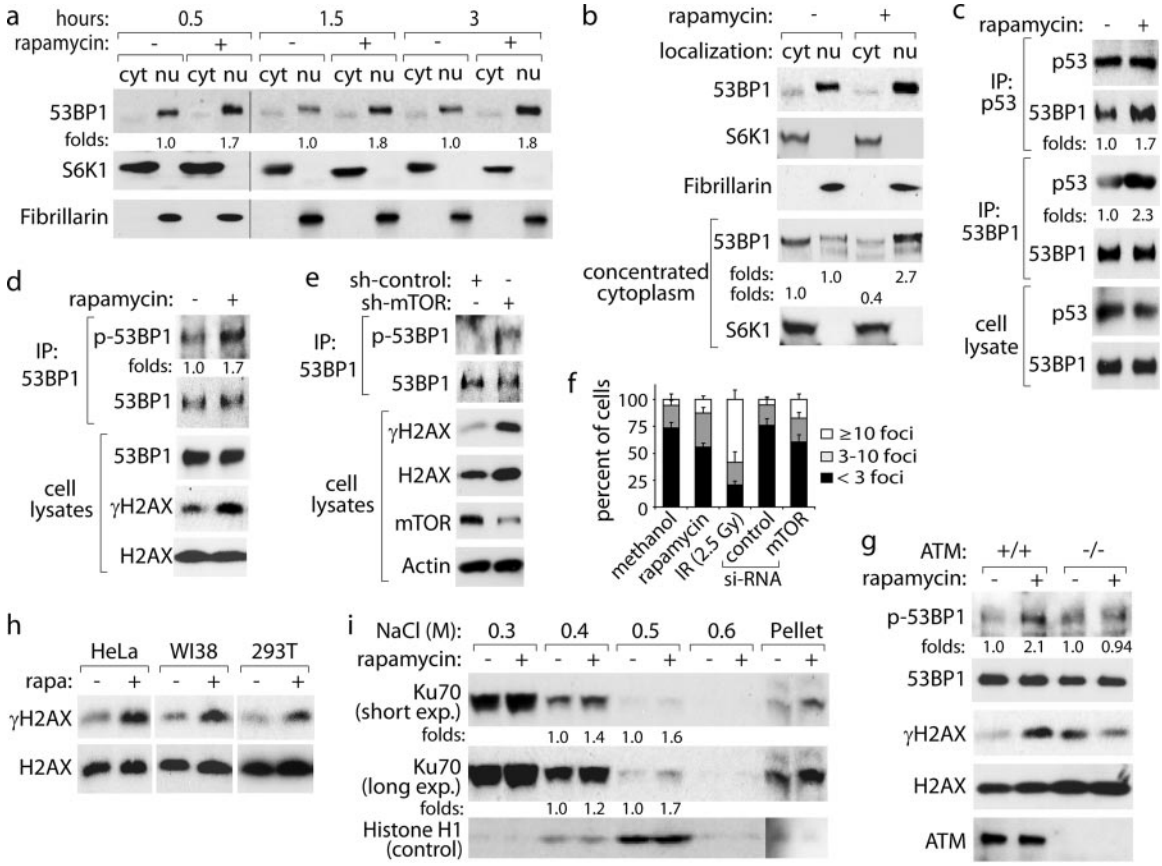

FIG. 3. **mTOR inhibition activates cellular DNA damage response pathways.** *a*, time course of the effects of rapamycin on nuclear (*nu*) and cytoplasmic (*cyt*) levels of 53BP1 in HeLa cells. -Fold changes for relative intensities of 53BP1 bands are given *below* the 53BP1 blot. *b*, nuclear and cytoplasmic levels of 53BP1 upon rapamycin treatment. The amount of cytoplasmic protein loaded was increased and nuclear protein amounts were proportionally decreased to test for translocation of 53BP1 by rapamycin. *c*, rapamycin enhances interaction between 53BP1 and p53. Immunoprecipitates (*IP*) were isolated from HeLa cells using either anti-p53 or anti-53BP1 antibody, and the amounts of associated 53BP1 and p53, respectively, were analyzed by Western blotting. *d* and *e*, rapamycin (3 h) and mTOR knockdown enhance phosphorylation of 53BP1 and H2AX in HeLa cells. *f*, rapamycin and mTOR silencing induced an increase in 53BP1 foci formation. HeLa cells treated with rapamycin/vehicle for 3 h or transduced with mTOR/control siRNA were monitored for the number of 53BP1 foci microscopically; error bars indicate calculated standard deviation from independent experiments. *g*, rapamycin induces phosphorylation of 53BP1 and H2AX in $ATM^{+/+}$ cells within 3 h but not in $ATM^{-/-}$ cells. *h*, rapamycin (*rapa*) induced H2AX phosphorylation in WI38 and 293T cells. *i*, rapamycin inhibits extraction of nuclear Ku70 by salt treatment in HeLa nuclear preparations. HeLa cells treated with rapamycin/methanol for 3 h were processed for Ku70 or histone H1 (control) extractability from nuclear fractions under increasing NaCl concentrations as indicated. *Numbers below* blots indicate relative band intensities as determined by the Image J software. *exp.*, exposure; *sh*, short hairpin.

pathways, we considered the potential effect on cellular DDR under these conditions. Initially, we focused on 53BP1 given its known role as an early sensor of DNA damage (28). Increased nuclear accumulation of 53BP1 was apparent as early as 30 min after rapamycin treatment (Fig. 3*a*). 53BP1 was not affected at its mRNA levels by rapamycin (supplemental Fig. 6). An increase of 53BP1 in nuclear fractions coincided with a barely detectable decrease in cytoplasmic fractions (Fig. 3*b*, *top panel*), whereas overall cellular levels demonstrated no change (Fig. 3*c*, *bottom panel*). To test whether rapamycin caused translocation of 53BP1 from the cytoplasm to the nucleus, we concentrated cytoplasmic proteins further and loaded increased protein amounts of cytoplasmic fractions and decreased protein amounts of nuclear fractions (while still maintaining equal protein amounts for cytoplasmic and nuclear fractions, respectively). Under these conditions, rapamycin-induced translocation of 53BP1 was evident (Fig. 3*b*, *bottom panel*). As part of a cellular DDR, 53BP1 cooperates with p53 (39, 40). Hence, we tested for potential effects of rapamycin on the 53BP1/p53 interaction via immunoprecipitation. Consistent with DDR activation, rapamycin enhanced association of 53BP1 with p53 (Fig. 3*c*).

The related kinases ATM and ATR are central to cellular DDR as they promote DNA repair and cell survival by phosphorylation of substrate proteins (28). As a measure of ATM/ATR activation, we monitored the effect of mTOR inhibition on phosphorylation of ATM/ATR substrates, $53BP1^{Ser\text{-}25/29}$ and $H2AX^{Ser\text{-}139}$ as well as formation of 53BP1 nuclear foci. Rapamycin and mTOR knockdown enhanced ATM/ATR-specific phosphorylation of $53BP1^{Ser\text{-}25/29}$ and $H2AX^{Ser\text{-}139}$ in HeLa

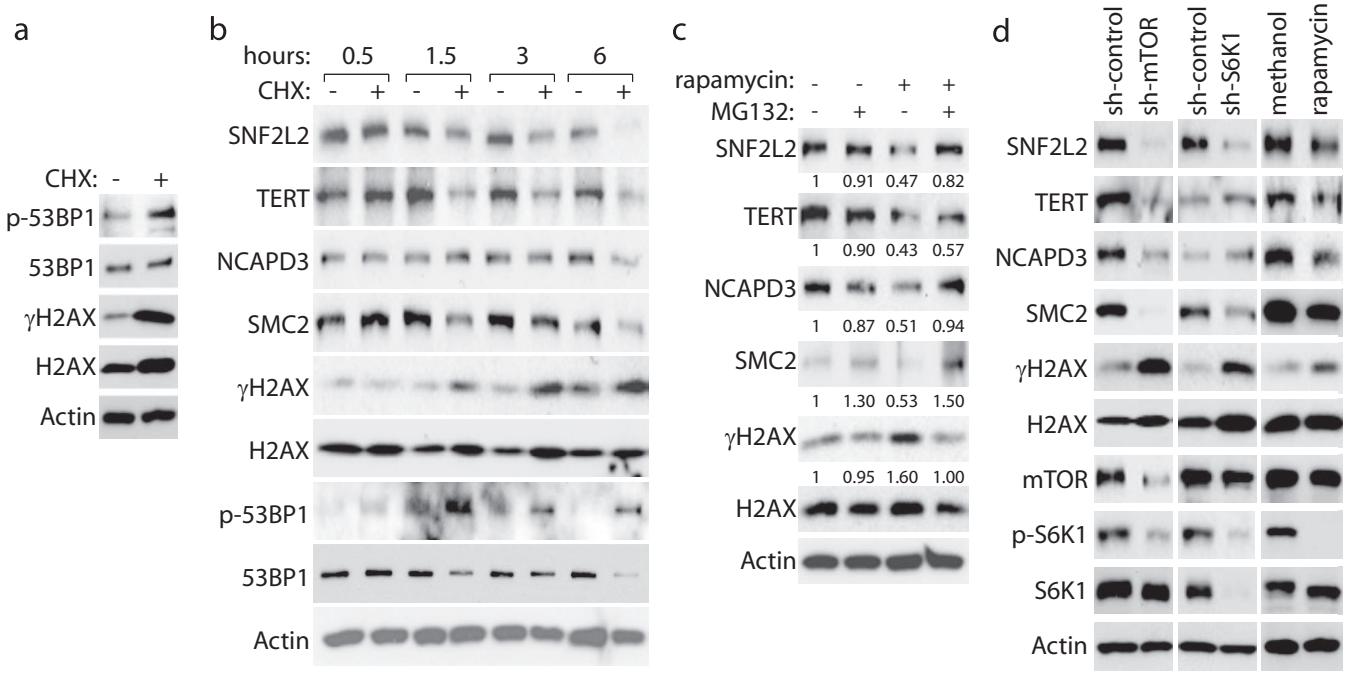

FIG. 4. **Rapamycin-induced changes are mimicked by protein synthesis inhibition.** *a*, effect of protein synthesis inhibitor cycloheximide (*CHX*; 50 μM, 90 min) on γ-H2AX and 53BP1 phosphorylation in HeLa cells. *b*, order of appearance of phosphorylation of 53BP1 and H2AX *versus* down-regulation of rapamycin-sensitive chromosomal integrity maintenance proteins upon cycloheximide treatment. Numbers indicate -fold changes in band intensities relative to those at no cycloheximide. *c*, effect of proteasomal inhibitor MG132 on rapamycin-induced phosphorylation of H2AX and down-regulation of the chromosomal integrity proteins. *d*, effect of mTOR knockdown, S6K1 knockdown, and 24 h of rapamycin treatment on levels of SNF2L2, TERT, NCAPD3, SMC2, and γ-H2AX.

cells (Fig. 3, *d* and *e*). mTOR inhibition and rapamycin treatment also produced a modest increase in the number of 53BP1 nuclear foci (Fig. 3*f*). Together, these results support the notion that mTOR inhibition activates DDR in HeLa cells. The ability of rapamycin to stimulate phosphorylation of 53BP1 and H2AX was seen in $ATM^{+/+}$ but not in $ATM^{-/-}$ lymphoblastic cells (Fig. 3*g*). Furthermore, rapamycin did not have any effect on ATR autophosphorylation in HeLa cells, implying that mTOR inhibition specifically activated ATM but not ATR signaling (supplemental Fig. 8). $H2AX^{Ser\text{-}139}$ phosphorylation was stimulated by rapamycin in at least two other cell lines, WI38 and 293T cells (Fig. 3*h*).

As a further test of DDR activation, we examined effects of rapamycin on recruitment of the DNA repair factor Ku70. ATM-dependent and -independent signaling causes recruitment of repair factors such as Ku70 to sites of DNA damage (41); this pool of Ku is relatively resistant to biochemical extraction (30). Supporting an activation of Ku proteins, we observed increased amounts of Ku70 extracted at higher concentrations of salt (0.4 M NaCl, 0.5 M NaCl, and pellet fractions) upon rapamycin treatment (Fig. 3*i*).

Collectively, the preceding results indicate that mTOR inhibition activated multiple steps of cellular DDR. Importantly, DDR-related phenotypes were apparent as early as 30 min (53BP1 phosphorylation; supplemental Fig. 9a) to 1.5 h (γ-H2AX phosphorylation; supplemental Fig. 9b) after rapamycin treatment, suggesting that these are unlikely to be related to potential effects of rapamycin on cell cycle progression.

Rapamycin-induced Activation of DDR Is Mimicked by Treatments That Inhibit Protein Synthesis and Suppressed by Proteasomal Inhibition—Next, we sought to understand how mTOR inhibition caused cellular DDR activation. Given that mTOR is a critical regulator of protein synthesis and translation, we investigated whether attenuating this cellular function might activate DDR/ATM signaling. Consistent with activated ATM signaling, a short pulse of treatment with the global protein synthesis inhibitor cycloheximide increased phosphorylation of $53BP1^{Ser\text{-}25/29}$ and $H2AX^{Ser\text{-}139}$ in HeLa cells (Fig. 4*a*). Similar results were also seen with amino acid starvation (supplemental Fig. 10), a treatment that inhibits mTOR and protein synthesis/translation (2, 42). Thus, protein synthesis inhibition is sufficient for cellular DDR activation, suggesting a potential basis for rapamycin-induced DDR. Attenuating protein synthesis would be expected to reduce overall protein levels (with proteins having relatively short half-lives, *i.e.* intrinsically unstable proteins being especially affected), including those that function to maintain chromosomal structure and/or operate within pathways of cellular DDR activation.

Interestingly, our proteomics analysis identified nuclear proteins involved in chromosomal integrity to be down-regulated upon rapamycin treatment (SNF2L2, TERT, NCAPD3, and SMC2; Fig. 1*c*) with no correlated effects on their mRNA levels (supplemental Fig. 6). Given the role of chromosomal

structure in the regulation of DDR pathways (43, 44) and the functions that the above mentioned set of proteins plays in maintaining chromosomal structure/integrity, one possibility is that their loss specifically triggered DDR upon rapamycin treatment.

To test whether the specific loss of rapamycin-sensitive chromosomal integrity proteins could activate DDR, we initially monitored the effect of a time course of cycloheximide treatment (Fig. 4*b*) on the levels of SNF2L2, TERT, NCAPD3, and SMC2 and their correlation with DDR activation (γ-H2AX and 53BP1 phosphorylation). SNF2L2, TERT, NCAPD3, and SMC2 decreased in overall abundance upon incubation of HeLa cells with cycloheximide for 1.5 h or longer; additionally, their decrease correlated well with increased phosphorylation of $H2AX^{Ser-139}$. However, 53BP1 phosphorylation occurred (by 30 min of cycloheximide treatment) substantially before the reduction in levels of SNF2L2, TERT, NCAPD3, and SMC2. Similarly, rapamycin-induced 53BP1 phosphorylation was apparent within 30 min of drug treatment, a time point at which there was no significant effect on the levels of SNF2L2, TERT, NCAPD3, and SMC2 (supplemental Fig. 9a). Thus, it appears unlikely that the specific reduction of the above mentioned chromosomal integrity proteins triggered DDR activation upon rapamycin treatment/mTOR inhibition. However, based on the known functions of these proteins, their reduced levels might play a role in sustaining DDR.

As an alternative, we tested whether stabilizing overall protein levels by proteasomal inhibition might affect rapamycin-induced phosphorylation of H2AX. As shown in Fig. 4*c*, co-treatment of cells with rapamycin and the proteasomal inhibitor MG132 suppressed H2AX phosphorylation. MG132 treatment also stabilized the levels of rapamycin-sensitive chromosomal integrity proteins, demonstrating that their steady-state levels are under proteasomal control. Thus, stabilization of proteins that might be intrinsically unstable (*i.e.* sensitive to attenuated protein synthesis/translation that follows mTOR inhibition) or potentially destabilized by mTOR inhibition is sufficient to suppress rapamycin-induced DDR activation. We anticipate that at least some of the rapamycin-sensitive proteins that are stabilized by proteasomal inhibition function in pathways of cellular DDR activation. Further work is necessary to identify rapamycin/protein synthesis-sensitive molecular candidates regulating DDR activation.

A major downstream effector of mTOR and a regulator of protein translation is S6K1 (1, 45). To further test for an involvement of protein synthesis inhibition in mTOR regulation of DDR, we tested the effect of S6K1 knockdown on steady-state levels of the nuclear proteins SNF2L2, TERT, NCAPD3, and SMC2 and the phosphorylation of H2AX. In contrast to what was seen upon prolonged rapamycin treatment or mTOR knockdown, S6K1 knockdown reduced the levels of SNF2L2 and SMC2 but not of TERT and NCAPD3 (Fig. 4*d*). Amino acid starvation, by contrast, did not affect levels of SNF2L2 and SMC2 (supplemental Fig. 10). Stable knockdown of either mTOR or S6K1 increased $H2AX^{Ser-139}$ phosphorylation, although this increase may be due to increases in the total levels of H2AX (Fig. 4*d*). Similar results were obtained from transient siRNA-based knockdown of mTOR or S6K1 (supplemental Fig. 11). Based on these findings, we infer that S6K1 has a partial role in mediating the effects of mTOR inhibition on cellular DDR activation.

Rapamcyin Pretreatment Enhances Radioresistance in HeLa Cells—Cells with activated DDR (either because of pre-exposure to stress or activating mutations) have a higher resistance to radiation or genotoxic stress (43, 46). Therefore, we tested for potential effects of rapamycin on cellular resistance to IR. Co-treatment of HeLa cells with rapamycin and IR had essentially no effect on cellular resistance compared with IR alone (Fig. 5*a*). In contrast, pretreatment of cells with rapamycin for 3 or 24 h prior to IR enhanced their survival rates, indicating a radioresistance effect (Fig. 5, *b* and *c*). A potential basis for this result is that rapamycin enhanced the ability of HeLa cells to repair DNA damage. Supporting this notion, we found that after pretreatment of cells with rapamycin for 3 or 24 h they accumulated lower levels of γ-H2AX upon subsequent exposure to increasing dosages of IR at 2.5 Gy or higher (Fig. 5*d*). This contrasts with the observation at lower doses of IR or in the absence of IR wherein rapamycin pretreatment increased γ-H2AX levels. Thus, rapamycin exerts a relatively modest effect on ATM activation compared with 2.5 Gy of IR (see also Fig. 3*f* showing substantially lower 53BP1 foci formation by rapamycin treatment *versus* 2.5 Gy of IR). However, rapamycin pretreatment activated a sufficiently broad DDR that enhances the ability of cells to reduce the effect of genotoxic stress on cell survival.

DISCUSSION

We have applied mass spectrometry-based proteomics to study mTOR regulation of the nuclear proteome, providing a panoramic snapshot of mTOR functions in the nucleus. Interestingly, several of the validated protein changes induced by rapamycin were not mirrored by changes in their corresponding mRNA levels with the only exception being TNKS1BP1 (supplemental Fig. 6). Thus, we identified several mTOR-regulated post-transcriptional events that would not have been detectable by transcriptomics or genomics approaches.

Additionally, our results provide a demonstration of the effectiveness of combining iTRAQ reagent stable isotope labeling and analysis using an LTQ linear ion trap mass spectrometer operated in PQD mode for a large scale quantitative proteomics study. We first described proof-of-principle studies demonstrating the potential for this method, which offers the powerful combination of multiplexed stable isotope labeling with a highly sensitive mass spectrometer (18, 25). Given the relatively small number of studies to date using the ion trap instrumentation for iTRAQ studies (47, 48), our results provide an important demonstration of the effectiveness of this method for large scale analysis within a complex sample,

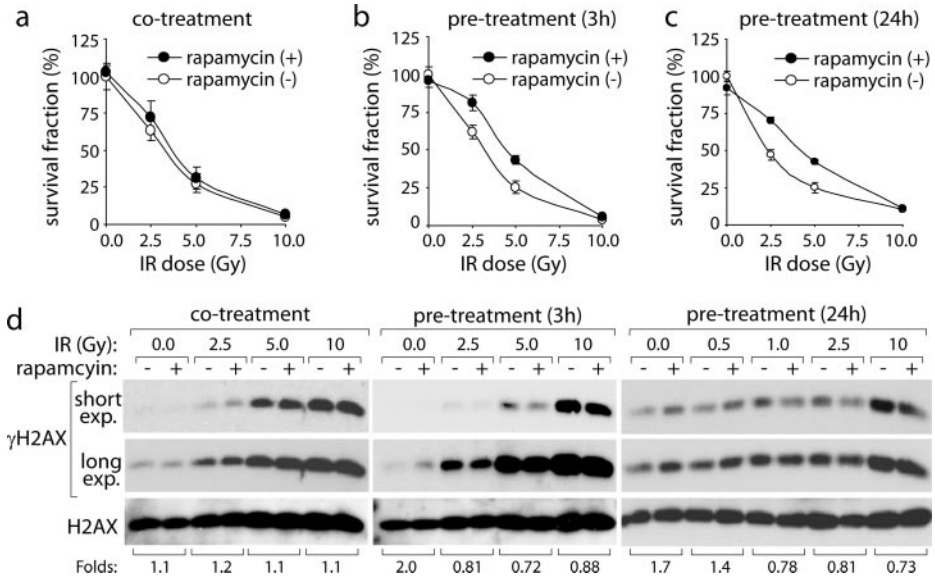

FIG. 5. **Pretreatment with rapamycin enhances resistance of HeLa cells to radiation.** HeLa cells treated with rapamycin/vehicle were exposed immediately to increasing doses of ionizing radiation (*a*) or after 3 (*b*) or 24 h (*c*) of pretreatment with rapamycin. Cell viability was measured as described under "Experimental Procedures." The effective doses of Gy to reduce the number of cell colonies by 50% were 3.44 ± 0.43 (rapamycin−) and 3.75 ± 0.32 Gy (rapamycin+) for co-treatment, 3.32 ± 0.24 (rapamycin−) and 4.88 ± 0.26 Gy (rapamycin+) for 3-h pretreatment, and 2.79 ± 0.19 (rapamycin−) and 4.39 ± 0.21 Gy (rapamycin+) for 24-h pretreatment. *d*, rapamycin-induced resistance to radiation (when cells were pretreated for 3 or 24 h) correlated with reduced accumulation of γ-H2AX in response to ionizing radiation. *Numbers below* the blots show -fold change in protein levels as determined by the Image J software. *exp.*, exposure.

supporting its value as a general tool for quantitative proteomics studies.

Our quantitative proteomics analysis revealed new nuclear functions regulated by mTOR. Specifically, the down-regulation of proteins involved in chromosomal integrity and an up-regulation of those involved in DDR upon rapamycin treatment pointed to a role for mTOR in regulating these functions in the cell. Given these unexpected findings, we focused on further characterizing this connection. Collectively, our observed effects on proteins involved in chromosomal integrity, ATM signaling, and the salt extractability of Ku70 (Figs. 1–3) suggest that mTOR inhibition putatively affects chromosomal structure and/or proteins that operate in pathways of cellular DDR activation. Several groups have documented that altered chromosomal structure is sufficient for activation of DDR pathways (43, 44). Using pulsed field electrophoresis, we were unable to detect direct DNA damage upon rapamycin treatment (data not shown), suggesting that the main effect of rapamycin/mTOR inhibition was on DDR activation rather than causing significant levels of DNA damage. Importantly, the effect mTOR inhibition on DDR activation is not a transient stress response but initiated early (supplemental Fig. 9) and sustained for at least 24 h of rapamycin treatment or longer (when mTOR is knocked down; Fig. 4*d*). Because chromosomal structure is an important determinant of gene expression, these effects could also explain how mTOR inhibition could potentially alter overall gene expression patterns and cellular processes in response to nutrients (5–7). In line with our results, rapamycin-sensitive and -insensitive branches of TOR signaling have been implicated in regulating chromosomal structure/functions in budding and fission yeasts (49, 50).

We suggest that activation of ATM by rapamycin depends on the steady-state level of currently unidentified critical proteins that function in pathways of cellular DDR activation. This is supported by our observation that proteasomal inhibition suppressed rapamycin-induced DDR, whereas translational attenuation by nutrient (amino acid starvation), molecular (S6K1 knockdown), and pharmacological (cycloheximide) treatments activated DDR. Based on the excellent agreement with cycloheximide treatment, we favor the notion that mTOR signaling regulates ATM via its effect on cellular protein synthesis machinery. However, potential regulation of proteasomal degradation pathways upon mTOR inhibition toward similar proteins also could contribute to ATM activation. Additional investigation is necessary to discriminate between these possibilities.

We also tested whether rapamycin treatment might activate AMPK, which in turn could lead to DDR activation. However, both short and long term treatment with rapamycin had no detectable effect on AMPK activation/phosphorylation, arguing against this possibility (supplemental Fig. 12).

Interestingly, all proteins up-regulated by rapamycin within the nucleus grouped within the functional category of DDR proteins. Among DDR proteins, we observed that rapamycin altered the ratio of abundance of 53BP1 between the cytoplasm and nucleus (Fig. 3*a*) but did not affect overall cellular levels of this protein. This implies that mammalian cells have

evolved mechanisms other than translation through which they transmit cytoplasmic signals of mTOR inhibition to the nucleus, reminiscent of the role played by yeast TOR in affecting nucleocytoplasmic relocalization events (1, 3). In contrast to 53BP1, subcellular relocalization is unlikely to account for increased abundance of TNKS1BP1 or the exclusively nuclear DDR proteins such as MDC1, NUP98, and NPM. One possibility is that rapamycin specifically stabilizes these proteins via inhibiting their degradation by the proteasome. However, this appears unlikely given the generally catabolic effects of rapamycin (1, 2) and its ability to enhance, rather than impede, proteasomal degradation of specific proteins (51, 52). An alternative possibility is that rapamycin enhances translation of transcripts corresponding to these DDR proteins via internal ribosome entry site/highly structured 5′-UTRs. Supporting such a possibility, the MFOLD algorithm (53) predicted strong secondary structures within the 5′-UTR of NPM1, NUP98, and MDC1 with ΔG values of −48.7, −148.3, and −170 kcal, respectively. TNKS1BP1 mRNA levels also increased upon rapamycin treatment, and supporting its potential for alternative translation, the 5′-UTR contains predicted strong secondary structure(s) ($\Delta G = -81.5$ kcal according to the MFOLD algorithm). These collective results point to a combination of mechanisms being likely involved in causing increased nuclear accumulation of DDR proteins upon rapamycin treatment.

The increased radioresistance of HeLa cells due to rapamycin indicates a positive effect of rapamycin on resistance to DNA damage (Fig. 5). The radioresistance was only observed with rapamycin pretreatment but not co-treatment with ionizing radiation, implying a time lag for signal amplification of the rapamycin-induced cellular response. Consistent with our observed inverse correlation between mTOR activity and radioresistance, previous studies demonstrated that mouse embryonic fibroblast cells deficient for the mTOR inhibitors *TSC1* and *TSC2* had a higher sensitivity to genotoxic agents, and rapamycin suppressed the sensitivity (54). However, this is not apparently a universal phenotype because variable effects of rapamycin/TOR inhibition on radio- or chemoresistance have been reported in different cell types and organisms (50, 55, 56). The relative balance between apoptotic induction and activation of cell survival and DDR pathways could represent a potential basis for these differences. Further work is necessary to elucidate the molecular basis for distinct effects of mTOR inhibition on different cell types. Regardless, the possibility that rapamycin/mTOR inhibition enhances radioresistance of some cancer cells has important implications for cancer treatments that combine genotoxic agents with mTOR inhibitors.

Collectively, our findings have potentially broad implications given that protein synthesis/TOR is emerging as an important determinant of aging and cancer (57, 58). Of note, recent studies indicated that defects in genome stability can trigger survival response similar to what is seen under calorie restriction or inhibition of insulin-like growth factor-1 signaling (59). These findings lie on the same line as our result that rapamycin-induced DDR activation enhanced survivability against DNA-damaging stresses. Several studies using model organisms revealed a positive effect of TOR inhibition or stress (at a moderate level) on lifespan extension (27). Our findings point to a possibility that rapamycin-induced activation of DDR or other changes in the nucleus may contribute to regulation of lifespan.

Acknowledgments—We thank J. H. Kweon for experimental help; E. Hendrickson and D. Clarke for comments on the manuscript; and Hendrickson, Griffin, and Kim laboratory members for comments and discussions.

* This work was supported, in whole or in part, by National Institutes of Health Grants DK072004 and P30 DK50456. This work was also supported by the Minnesota Medical Foundation, American Diabetes Association Grant 7-07-CD-08, and United States Department of Defense Grant TS060035.

S The on-line version of this article (available at http://www.mcponline.org) contains supplemental Figs. 1–12 and Tables 1–3.

§ Both authors contributed equally to this work.

‖ To whom correspondence may be addressed: Dept. of Biochemistry, Molecular Biology, and Biophysics, University of Minnesota, 6-155 Jackson Hall, 321 Church St. S. E., Minneapolis, MN 55455. Tel.: 612-626-3418; E-mail: dhkim@umn.edu.

** To whom correspondence may be addressed: Dept. of Biochemistry, Molecular Biology, and Biophysics, University of Minnesota, 6-155 Jackson Hall, 321 Church St. S. E., Minneapolis, MN 55455. Tel.: 612-624-5249; Fax: 612-624-0432; E-mail: tgriffin@umn.edu.

REFERENCES

1. Wullschleger, S., Loewith, R., and Hall, M. N. (2006) TOR signaling in growth and metabolism. *Cell* **124,** 471–484
2. Shamji, A. F., Nghiem, P., and Schreiber, S. L. (2003) Integration of growth factor and nutrient signaling: implications for cancer biology. *Mol. Cell* **12,** 271–280
3. Beck, T., and Hall, M. N. (1999) The TOR signalling pathway controls nuclear localization of nutrient-regulated transcription factors. *Nature* **402,** 689–692
4. Li, H., Tsang, C. K., Watkins, M., Bertram, P. G., and Zheng, X. F. (2006) Nutrient regulates Tor1 nuclear localization and association with rDNA promoter. *Nature* **442,** 1058–1061
5. Grolleau, A., Bowman, J., Pradet-Balade, B., Puravs, E., Hanash, S., Garcia-Sanz, J. A., and Beretta, L. (2002) Global and specific translational control by rapamycin in T cells uncovered by microarrays and proteomics. *J. Biol. Chem.* **277,** 22175–22184
6. Guertin, D. A., Guntur, K. V., Bell, G. W., Thoreen, C. C., and Sabatini, D. M. (2006) Functional genomics identifies TOR-regulated genes that control growth and division. *Curr. Biol.* **16,** 958–970
7. Peng, T., Golub, T. R., and Sabatini, D. M. (2002) The immunosuppressant rapamycin mimics a starvation-like signal distinct from amino acid and glucose deprivation. *Mol. Cell. Biol.* **22,** 5575–5584
8. Park, I. H., Bachmann, R., Shirazi, H., and Chen, J. (2002) Regulation of ribosomal S6 kinase 2 by mammalian target of rapamycin. *J. Biol. Chem.* **277,** 31423–31429
9. Kim, J. E., and Chen, J. (2000) Cytoplasmic-nuclear shuttling of FKBP12-rapamycin-associated protein is involved in rapamycin-sensitive signaling and translation initiation. *Proc. Natl. Acad. Sci. U.S.A.* **97,** 14340–14345
10. Bernardi, R., Guernah, I., Jin, D., Grisendi, S., Alimonti, A., Teruya-Feldstein, J., Cordon-Cardo, C., Simon, M. C., Rafii, S., and Pandolfi, P. P. (2006) PML inhibits HIF-1alpha translation and neoangiogenesis through repression of mTOR. *Nature* **442,** 779–785
11. Yang, T. T., Yu, R. Y., Agadir, A., Gao, G. J., Campos-Gonzalez, R., Tournier, C., and Chow, C. W. (2008) Integration of protein kinases

mTOR and extracellular signal-regulated kinase 5 in regulating nucleocytoplasmic localization of NFATc4. *Mol. Cell. Biol.* **28,** 3489–3501
12. Porstmann, T., Santos, C. R., Griffiths, B., Cully, M., Wu, M., Leevers, S., Griffiths, J. R., Chung, Y. L., and Schulze, A. (2008) SREBP activity is regulated by mTORC1 and contributes to Akt-dependent cell growth. *Cell Metab.* **8,** 224–236
13. Mayer, C., Bierhoff, H., and Grummt, I. (2005) The nucleolus as a stress sensor: JNK2 inactivates the transcription factor TIF-IA and down-regulates rRNA synthesis. *Genes Dev.* **19,** 933–941
14. Ideker, T., Thorsson, V., Ranish, J. A., Christmas, R., Buhler, J., Eng, J. K., Bumgarner, R., Goodlett, D. R., Aebersold, R., and Hood, L. (2001) Integrated genomic and proteomic analyses of a systematically perturbed metabolic network. *Science* **292,** 929–934
15. Griffin, T. J., Gygi, S. P., Ideker, T., Rist, B., Eng, J., Hood, L., and Aebersold, R. (2002) Complementary profiling of gene expression at the transcriptome and proteome levels in Saccharomyces cerevisiae. *Mol. Cell. Proteomics* **1,** 323–333
16. Washburn, M. P., Koller, A., Oshiro, G., Ulaszek, R. R., Plouffe, D., Deciu, C., Winzeler, E., and Yates, J. R., 3rd (2003) Protein pathway and complex clustering of correlated mRNA and protein expression analyses in Saccharomyces cerevisiae. *Proc. Natl. Acad. Sci. U.S.A.* **100,** 3107–3112
17. Yates, J. R., Ruse, C. I., and Nakorchevsky, A. (2009) Proteomics by mass spectrometry: approaches, advances, and applications. *Annu. Rev. Biomed. Eng.* **11,** 49–79
18. Griffin, T. J., Xie, H., Bandhakavi, S., Popko, J., Mohan, A., Carlis, J. V., and Higgins, L. (2007) iTRAQ reagent-based quantitative proteomic analysis on a linear ion trap mass spectrometer. *J. Proteome Res.* **6,** 4200–4209
19. Eng, J., McCormack, A. L., and Yates, J. R., 3rd (1994) An approach to correlate tandem mass spectral data of peptides with amino acid sequences in a protein database. *J. Am. Soc. Mass Spectrom.* **5,** 976–989
20. Peng, J., Elias, J. E., Thoreen, C. C., Licklider, L. J., and Gygi, S. P. (2003) Evaluation of multidimensional chromatography coupled with tandem mass spectrometry (LC/LC-MS/MS) for large-scale protein analysis: the yeast proteome. *J. Proteome Res.* **2,** 43–50
21. Keller, A., Nesvizhskii, A. I., Kolker, E., and Aebersold, R. (2002) Empirical statistical model to estimate the accuracy of peptide identifications made by MS/MS and database search. *Anal. Chem.* **74,** 5383–5392
22. Han, D. K., Eng, J., Zhou, H., and Aebersold, R. (2001) Quantitative profiling of differentiation-induced microsomal proteins using isotope-coded affinity tags and mass spectrometry. *Nat. Biotechnol.* **19,** 946–951
23. Sancak, Y., Peterson, T. R., Shaul, Y. D., Lindquist, R. A., Thoreen, C. C., Bar-Peled, L., and Sabatini, D. M. (2008) The Rag GTPases bind raptor and mediate amino acid signaling to mTORC1. *Science* **320,** 1496–1501
24. Masutomi, K., Yu, E. Y., Khurts, S., Ben-Porath, I., Currier, J. L., Metz, G. B., Brooks, M. W., Kaneko, S., Murakami, S., DeCaprio, J. A., Weinberg, R. A., Stewart, S. A., and Hahn, W. C. (2003) Telomerase maintains telomere structure in normal human cells. *Cell* **114,** 241–253
25. Meany, D. L., Xie, H., Thompson, L. V., Arriaga, E. A., and Griffin, T. J. (2007) Identification of carbonylated proteins from enriched rat skeletal muscle mitochondria using affinity chromatography-stable isotope labeling and tandem mass spectrometry. *Proteomics* **7,** 1150–1163
26. Kuwahata, M., Yoshimura, T., Sawai, Y., Amano, S., Tomoe, Y., Segawa, H., Tatsumi, S., Ito, M., Ishizaki, S., Ijichi, C., Sonaka, I., Oka, T., and Miyamoto, K. (2008) Localization of polypyrimidine-tract-binding protein is involved in the regulation of albumin synthesis by branched-chain amino acids in HepG2 cells. *J. Nutr. Biochem.* **19,** 438–447
27. Spellman, R., Llorian, M., and Smith, C. W. (2007) Crossregulation and functional redundancy between the splicing regulator PTB and its paralogs nPTB and ROD1. *Mol. Cell* **27,** 420–434
28. Hurley, P. J., and Bunz, F. (2007) ATM and ATR: components of an integrated circuit. *Cell Cycle* **6,** 414–417
29. Seimiya, H., and Smith, S. (2002) The telomeric poly(ADP-ribose) polymerase, tankyrase 1, contains multiple binding sites for telomeric repeat binding factor 1 (TRF1) and a novel acceptor, 182-kDa tankyrase-binding protein (TAB182). *J. Biol. Chem.* **277,** 14116–14126
30. Lee, S. Y., Park, J. H., Kim, S., Park, E. J., Yun, Y., and Kwon, J. (2005) A proteomics approach for the identification of nucleophosmin and heterogeneous nuclear ribonucleoprotein C1/C2 as chromatin-binding proteins in response to DNA double-strand breaks. *Biochem. J.* **388,** 7–15
31. Wang, G. G., Cai, L., Pasillas, M. P., and Kamps, M. P. (2007) NUP98-NSD1 links H3K36 methylation to Hox-A gene activation and leukaemogenesis. *Nat. Cell. Biol.* **9,** 804–812
32. Jiang, S., Meyer, R., Kang, K., Osborne, C. K., Wong, J., and Oesterreich, S. (2006) Scaffold attachment factor SAFB1 suppresses estrogen receptor alpha-mediated transcription in part via interaction with nuclear receptor corepressor. *Mol. Endocrinol.* **20,** 311–320
33. Sergeant, K. A., Bourgeois, C. F., Dalgliesh, C., Venables, J. P., Stevenin, J., and Elliott, D. J. (2007) Alternative RNA splicing complexes containing the scaffold attachment factor SAFB2. *J. Cell Sci.* **120,** 309–319
34. Racki, L. R., and Narlikar, G. J. (2008) ATP-dependent chromatin remodeling enzymes: two heads are not better, just different. *Curr. Opin. Genet. Dev.* **18,** 137–144
35. Hagstrom, K. A., and Meyer, B. J. (2003) Condensin and cohesin: more than chromosome compactor and glue. *Nat. Rev. Genet.* **4,** 520–534
36. Braun, R. J., and Zischka, H. (2008) Mechanisms of Cdc48/VCP-mediated cell death: from yeast apoptosis to human disease. *Biochim. Biophys. Acta* **1783,** 1418–1435
37. Bae-Jump, V. L., Zhou, C., Gehrig, P. A., Whang, Y. E., and Boggess, J. F. (2006) Rapamycin inhibits hTERT telomerase mRNA expression, independent of cell cycle arrest. *Gynecol. Oncol.* **100,** 487–494
38. Zhou, C., Gehrig, P. A., Whang, Y. E., and Boggess, J. F. (2003) Rapamycin inhibits telomerase activity by decreasing the hTERT mRNA level in endometrial cancer cells. *Mol. Cancer Ther.* **2,** 789–795
39. Wang, B., Matsuoka, S., Carpenter, P. B., and Elledge, S. J. (2002) 53BP1, a mediator of the DNA damage checkpoint. *Science* **298,** 1435–1438
40. Ward, I. M., Difilippantonio, S., Minn, K., Mueller, M. D., Molina, J. R., Yu, X., Frisk, C. S., Ried, T., Nussenzweig, A., and Chen, J. (2005) 53BP1 cooperates with p53 and functions as a haploinsufficient tumor suppressor in mice. *Mol. Cell. Biol.* **25,** 10079–10086
41. Drouet, J., Frit, P., Delteil, C., de Villartay, J. P., Salles, B., and Calsou, P. (2006) Interplay between Ku, Artemis, and the DNA-dependent protein kinase catalytic subunit at DNA ends. *J. Biol. Chem.* **281,** 27784–27793
42. Kimball, S. R., and Jefferson, L. S. (2005) Role of amino acids in the translational control of protein synthesis in mammals. *Semin. Cell Dev. Biol.* **16,** 21–27
43. Murga, M., Jaco, I., Fan, Y., Soria, R., Martinez-Pastor, B., Cuadrado, M., Yang, S. M., Blasco, M. A., Skoultchi, A. I., and Fernandez-Capetillo, O. (2007) Global chromatin compaction limits the strength of the DNA damage response. *J. Cell Biol.* **178,** 1101–1108
44. Bakkenist, C. J., and Kastan, M. B. (2003) DNA damage activates ATM through intermolecular autophosphorylation and dimer dissociation. *Nature* **421,** 499–506
45. Jastrzebski, K., Hannan, K. M., Tchoubrieva, E. B., Hannan, R. D., and Pearson, R. B. (2007) Coordinate regulation of ribosome biogenesis and function by the ribosomal protein S6 kinase, a key mediator of mTOR function. *Growth Factors* **25,** 209–226
46. Kelsey, K. T., Memisoglu, A., Frenkel, D., and Liber, H. L. (1991) Human lymphocytes exposed to low doses of X-rays are less susceptible to radiation-induced mutagenesis. *Mutat. Res.* **263,** 197–201
47. Armenta, J. M., Hoeschele, I., and Lazar, I. M. (2009) Differential protein expression analysis using stable isotope labeling and PQD linear ion trap MS technology. *J. Am. Soc. Mass Spectrom.* **20,** 1287–1302
48. Yang, F., Wu, S., Stenoien, D. L., Zhao, R., Monroe, M. E., Gritsenko, M. A., Purvine, S. O., Polpitiya, A. D., Toliæ, N., Zhang, Q., Norbeck, A. D., Orton, D. J., Moore, R. J., Tang, K., Anderson, G. A., Pasa-Toliæ, L., Camp, D. G., 2nd, and Smith, R. D. (2009) Combined pulsed-Q dissociation and electron transfer dissociation for identification and quantification of iTRAQ-labeled phosphopeptides. *Anal. Chem.* **81,** 4137–4143
49. Tsang, C. K., Bertram, P. G., Ai, W., Drenan, R., and Zheng, X. F. (2003) Chromatin-mediated regulation of nucleolar structure and RNA Pol I localization by TOR. *EMBO J.* **22,** 6045–6056
50. Schonbrun, M., Laor, D., López-Maury, L., Bähler, J., Kupiec, M., and Weisman, R. (2009) TOR complex 2 controls gene silencing, telomere length maintenance and survival under DNA damaging conditions. *Mol. Cell. Biol.* **29,** 4584–4594
51. García-Morales, P., Hernando, E., Carrasco-García, E., Menéndez-Gutierrez, M. P., Saceda, M., and Martínez-Lacaci, I. (2006) Cyclin D3 is down-regulated by rapamycin in HER-2-overexpressing breast cancer cells. *Mol. Cancer Ther.* **5,** 2172–2181
52. Jin, H. K., Ahn, S. H., Yoon, J. W., Park, J. W., Lee, E. K., Yoo, J. S., Lee, J. C., Choi, W. S., and Han, J. W. (2009) Rapamycin down-regulates

inducible nitric oxide synthase by inducing proteasomal degradation. *Biol. Pharm. Bull.* **32,** 988–992
53. Zuker, M. (2003) Mfold web server for nucleic acid folding and hybridization prediction. *Nucleic Acids Res.* **31,** 3406–3415
54. Ghosh, S., Tergaonkar, V., Rothlin, C. V., Correa, R. G., Bottero, V., Bist, P., Verma, I. M., and Hunter, T. (2006) Essential role of tuberous sclerosis genes TSC1 and TSC2 in NF-kappaB activation and cell survival. *Cancer Cell* **10,** 215–226
55. Paglin, S., Lee, N. Y., Nakar, C., Fitzgerald, M., Plotkin, J., Deuel, B., Hackett, N., McMahill, M., Sphicas, E., Lampen, N., and Yahalom, J. (2005) Rapamycin-sensitive pathway regulates mitochondrial membrane potential, autophagy, and survival in irradiated MCF-7 cells. *Cancer Res.* **65,** 11061–11070
56. Beuvink, I., Boulay, A., Fumagalli, S., Zilbermann, F., Ruetz, S., O'Reilly, T., Natt, F., Hall, J., Lane, H. A., and Thomas, G. (2005) The mTOR inhibitor RAD001 sensitizes tumor cells to DNA-damaged induced apoptosis through inhibition of p21 translation. *Cell* **120,** 747–759
57. Tavernarakis, N. (2008) Ageing and the regulation of protein synthesis: a balancing act? *Trends Cell Biol.* **18,** 228–235
58. Harrison, D. E., Strong, R., Sharp, Z. D., Nelson, J. F., Astle, C. M., Flurkey, K., Nadon, N. L., Wilkinson, J. E., Frenkel, K., Carter, C. S., Pahor, M., Javors, M. A., Fernandez, E., and Miller, R. A. (2009) Rapamycin fed late in life extends lifespan in genetically heterogeneous mice. *Nature* **460,** 392–395
59. Schumacher, B., Hoeijmakers, J. H., and Garinis, G. A. (2009) Sealing the gap between nuclear DNA damage and longevity. *Mol. Cell. Endocrinol.* **299,** 112–117